A theoretical study on ionization of ethylene with analysis of vibrational structure of the photoelectron spectra

Kouichi Takeshita[a)]
Department of Chemistry, Faculty of Science, Hokkaido University, Sapporo 060 Japan

(Received 5 September 1990; accepted 16 April 1991)

Ab initio calculations have been performed to study the vibrational levels of the low-lying ionic states, $^2B_{3u}$, $^2B_{3g}$, ^2A_g, $^2B_{2u}$, and $^2B_{1u}$ of ethylene. The equilibrium molecular structure and vibrational modes of these states are presented. The theoretical ionization intensity curve including the vibrational structure is also presented and compared with the photoelectron spectra of C_2H_4 and C_2D_4. A number of new assignments of the photoelectron spectra are proposed.

I. INTRODUCTION

The electronic ground state of ethylene is represented by a configuration $\cdots(2b_{1u})^2(1b_{2u})^2(3a_g)^2(1b_{3g})^2(1b_{3u})^2$ with the D_{2h} symmetry point group. The totally symmetric vibrational modes of ν_1, ν_2, and ν_3 are assigned to the C–H stretching, C–C stretching, and H–C–H bending modes, respectively.

The experimental investigation of cationic states of ethylene have been performed by means of the 584 Å photoelectron (PE) spectra. The PE spectra of C_2H_4 and C_2D_4 have been observed in the energy range from 10.5 to 20 eV.[1–5] The spectrum consists of five bands which are assigned to the $^2B_{3u}$, $^2B_{3g}$, ^2A_g, $^2B_{2u}$, and $^2B_{1u}$ states from the lower energy side.

The assignment of the vibrational structure of each band has been reported by many observers. Pollard *et al.*[5] and Dehmer *et al.*[6] have discussed the vibrational structure of the first band which includes the torsional mode. The assignments of the vibrational structure of the second, third, and fourth bands by Branton *et al.*[1,2] and Pollard *et al.*[5] disagree with each other. The well-resolved fourth band has been interpreted as the vibrational structure at a saddle point in the potential surface by Pollard *et al.*[5] As far as we know, no discussion on the vibrational levels of the fifth band has been reported.

Theoretical investigations for the first ionic state have been reported in connection with the molecular structure[7–10] and torsional potential surface.[11,12] Somasundran *et al.*[9] have reported the vibrational frequencies of the first ionic state. Köppel *et al.*[13,14] have reported the vibronic coupling effects of the lowest two ionic states in the photoelectron spectrum.

As the molecule is ionized, the equilibrium molecular structure and the vibrational mode are changed from those of the ground state. The vibrational structure of the PE spectrum reflects these changes. It is therefore interesting to investigate the vibrational structure associated with the change in the equilibrium molecular structure and the vibrational mode by ionization. The *ab initio* calculations on the equilibrium molecular structure and vibrational modes of C_2H_4 have been reported.[7–12] However, many authors have had interest in the first and second ionic states. No *ab initio* investigation of the equilibrium molecular structure and vibrational structure of the higher bands has been reported.

In this work, we determined the equilibrium molecular structure of the ground and lowest five ionic states by using the *ab initio* self-consistent-field (SCF) method. We also studied the potential surface of the torsional angle by means of the configuration interaction method. Within the framework of the adiabatic approximation and the harmonic oscillator approximation, we calculated the harmonic force constant matrix elements over variables of the totally symmetric distortion of the D_{2h} symmetry and the vibrational frequencies of the totally symmetric modes. We obtained approximate theoretical intensity curves using the Franck–Condon factor (FCF) which is given by the square of the overlap integrals between the vibrational wave function of the ground state and that of the ionic state. Based on these calculations, we discuss the vibrational levels of the low-lying five ionic states compared to the photoelectron spectra of C_2H_4 and C_2D_4.

II. METHOD OF CALCULATIONS

The basis set of C is obtained by contracting Duijneveldt's[15] Gaussian-type orbitals (10*s*5*p*) to [5*s*3*p*]. The contraction scheme is given by Shoda.[16] Two *d* type polarization functions with exponents of 1.10 and 0.31 are augmented. The basis set of H is obtained by contracting Duijneveldt's Gaussian-type orbitals (5*s*) to [3*s*], which is augmented with one *p*-type polarization function with exponent 0.95.

The gradient technique for the Roothaan's restricted-Hartree–Fock (RHF) method was applied to determine the optimum molecular structure of the ground and lowest five ionic states with restriction of D_{2h} symmetry.

The single and double excitation configuration interaction (SDCI) calculations were carried out to obtain accurate ionization energies and the torsional potential surfaces. Using an SCF wave function of the respective state [see Table I(a)] as a single reference configuration, singly and doubly excited configuration state functions (CSFs) were generated where the *K* shell electrons of C were kept frozen. The

a) Present address: Faculty of Bioindustry, Tokyo University of Agriculture, Abashiri, Hokkaido 099-24, Japan.

 0021-9606/91/151838-09$03.00

TABLE I. Reference function and the number of configuration state functions with (a) D_{2h} symmetry and (b) D_2 symmetry.

(a)	State	Reference function	#CSF
	^1A_g	$\cdots(2b_{1u})^2(1b_{2u})^2(3a_g)^2(1b_{3g})^2(1b_{3u})^2$	10 441
	$^2B_{3u}$	$\cdots(2b_{1u})^2(1b_{2u})^2(3a_g)^2(1b_{3g})^2(1b_{3u})^1$	10 246
	$^2B_{3g}$	$\cdots(2b_{1u})^2(1b_{2u})^2(3a_g)^2(1b_{3g})^1(1b_{3u})^2$	10 352
	^2A_g	$\cdots(2b_{1u})^2(1b_{2u})^2(3a_g)^1(1b_{3g})^2(1b_{3u})^2$	10 367
	$^2B_{2u}$	$\cdots(2b_{1u})^2(1b_{2u})^1(3a_g)^2(1b_{3g})^2(1b_{3u})^2$	10 352
	$^2B_{1u}$	$\cdots(2b_{1u})^1(1b_{2u})^2(3a_g)^2(1b_{3g})^2(1b_{3u})^2$	10 370
(b)	State	Reference function	#CSF
	^1A	$\cdots(2b_1)^2(1b_2)^2(3a)^2(2b_3)^2$	18 722
	$1\,^2B_3$	$\cdots(2b_1)^2(1b_2)^2(3a)^2(2b_3)^1$	18 653
	$2\,^2B_3$	$\cdots(2b_1)^2(1b_2)^2(3a)^2(2b_3)^1$	35 632
		$\cdots(2b_1)^2(1b_2)^2(3a)^2(1b_3)^1(2b_3)^2$	
	^2A	$\cdots(2b_1)^2(1b_2)^2(3a)^1(2b_3)^2$	18 653
	$^2B_2$	$\cdots(2b_1)^2(1b_2)^1(3a)^2(2b_3)^2$	18 656
	$^2B_1$	$\cdots(2b_1)^1(1b_2)^2(3a)^2(2b_3)^2$	18 656

generated CSFs were restricted to the first order interacting space.[17] The number of the generated CSFs of each state is also shown in Table I(a). The torsional potential surfaces were calculated by the use of the D_2 symmetry. The reference CSF and the number of the generated CSFs of each state are shown in Table I(b). The contribution of quadruple excitations was estimated by means of the Langhoff and Davidson's correction method.[18] As the dimension of the CI of the second $^2B_3$ state is too large, we have adopted a CSF selection process by the use of second-order perturbation theory. The threshold for the selection was 1 μhartree. The dimension of the Hamiltonian matrix was then reduced to 15 764 at the planar structure. We have estimated the total energy including the contribution from the rejected CSFs by second-order perturbation theory.[19]

The harmonic force constant matrix elements were calculated by means of the gradient technique with an RHF wave function; the second derivative was estimated by the numerical differentiation of the analytically calculated first derivative. We calculated the FCFs of only the totally symmetric vibrational modes. In calculating FCFs, we approximated the vibrational wave functions by those obtained by the harmonic oscillatory model. We assumed that the initial state was the zero point vibrational level of the ground state. The method of calculation of the FCF and theoretical intensity curves was the same as we used in the previous paper.[20]

This work has been carried out by using the computer program system GRAMOL[21] for the gradient technique and the calculation of normal modes, and MICA3[22] for the CI calculations.

III. RESULTS AND DISCUSSION

The results of the optimized molecular structure of the ground and ionic states by the use of the SCF method are listed in Table II. The results of the ground and $^2B_{3u}$ states are in good agreement with the calculated values by Somasundran *et al.*[9] (see Table II) at the SCF/(5*s*4*p*2*d*/3*s*1*p*) level. The magnitude of the change in geometry by ionization is also presented in parenthesis in Table II.

TABLE II. Optimized geometry and change in geometry by ionization.[a]

State	C–C(ΔC–C)	C–H (ΔC–H)	H–C–H (ΔH–C–H)
^1A_g	1.314	1.074	116.74
$^2B_{3u}$	1.401(+ 0.087)	1.075(+ 0.001)	118.70(+ 1.96)
$^2B_{3g}$	1.245(− 0.069)	1.127(+ 0.053)	100.86(− 15.88)
^2A_g	1.429(+ 0.115)	1.079(+ 0.005)	140.76(+ 24.02)
$^2B_{2u}$	1.333(+ 0.019)	1.134(+ 0.060)	100.04(− 16.70)
$^2B_{1u}$	1.269(− 0.045)	1.152(+ 0.078)	126.80(+ 10.06)

[a] Bond lengths are in angstroms, angles in degrees. The values in parenthesis are the magnitude of the change in geometry by ionization. Somasundran *et al.* (Ref. 9) have reported the optimized geometry of ^1A_g and $^2B_{3u}$ as following; for ^1A_g, C–C = 1.3143 Å, C–H = 1.0748 Å, and H–C–H = 116.679°, for $^2B_{3u}$, C–C = 1.4000 Å, C_1–H_1 = 1.0755 Å, C_1–H_2 = 1.0756 Å, C_2–H_3 = 1.0755 Å, C_2–H_4 = 1.0755 Å, H_1–C_1–H_1 = 118.649° and H_3–C_2–H_4 = 118.579°.

In order to examine the stability of the planar structure, we calculated the potential surface vs torsional angle where the other internal coordinates were restricted to those obtained at the planar structure. The $^2B_{3u}$, $^2B_{3g}$, ^2A_g, $^2B_{2u}$, and $^2B_{1u}$ states of a planar D_{2h} structure are correlated with the first $^2B_3$ ($1\,^2B_3$), second $^2B_3$ ($2\,^2B_3$), ^2A, $^2B_2$, and $^2B_1$ states of none planar D_2 structure, respectively. Figure 1 shows the torsional potential surfaces of the first $^2B_3$ state by means of the RHF, SDCI and its quadruple correction (QC) by Langhoff and Davidson's method. The potential surface estimated by the QC method gives a twisted equilibrium struc-

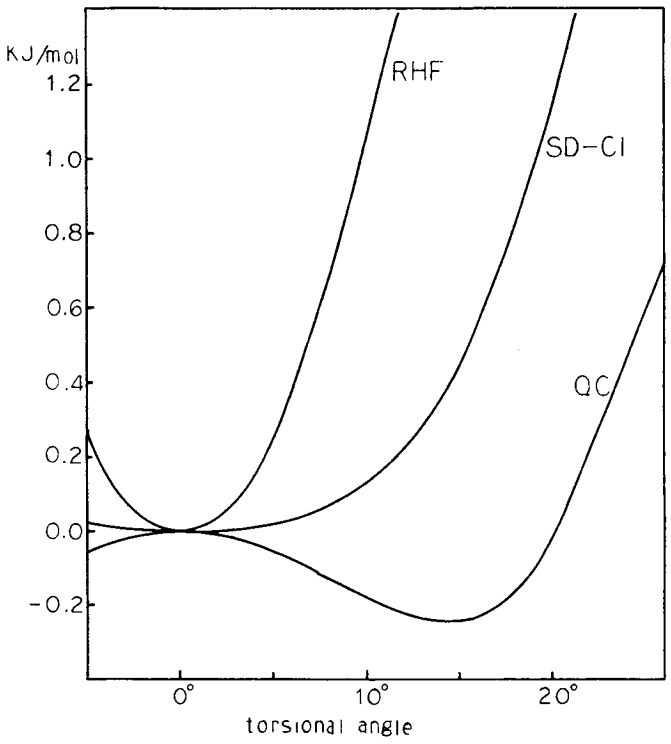

FIG. 1. The torsional potential surfaces of the lowest $^2B_3$ state by means of the RHF, SDCI and its quadruple correction (QC) by Langhoff and Davidson's method (Ref. 18) methods.

ture for this state. Figure 1 shows that the equilibrium twisted angle is 14° and this structure is lying 0.25 KJ/mol below the planar structure. Handy *et al.*[12] have shown that a highly correlated wave function with a very large basis set is necessary to describe even qualitatively the torsional potential function of the first state. They obtained the equilibrium twisted angle of 16° and the torsional stabilization energy of 0.4 KJ/mol by the CEPA/6-311G(*d,p*) level. From experiment Köppel *et al.*[13] deduced the twisting angle to be 25° and the torsional barrier to be 2.8 KJ/mol. The torsional potential surfaces of the 2 $^2B_3$, ^2A, $^2B_2$, and $^2B_1$ states by the use of the three methods, however, amount to planar equilibrium geometry. The result of the fourth state ($^2B_2$) disagrees with that of Sannen *et al.*[11] They reported that the surface of the fourth state has a saddle point at the planar geometry based on the single excitation method with MO basis set obtained from the ground state of the neutral molecule.

The total energies by the SCF and SDCI methods at the optimized ground state geometry and the vertical ionization energies (VIEs) are given in Table III. The total energies at the optimized geometries of the ionic states and the adiabatic ionization energies (AIEs) are shown in Table IV. The AIEs of the $^2B_{3u}$, $^2B_{3g}$, ^2A_g, $^2B_{2u}$, and $^2B_{1u}$ states obtained by the SDCI method are lower than the VIEs by 0.25, 0.52, 0.97, 0.68, and 0.53 eV, respectively. The weights of the reference function in the SDCI calculations are also given in parentheses. The VIEs and AIEs including the quadruple correction energy are also listed in Table III and IV, respectively.

Table V(a) contains the calculated vibrational frequencies of the totally symmetric modes of the ground and ionic states of C_2H_4 by the use of the RHF wave functions. The vibrational frequencies of C_2D_4 are listed in Table V(b). Comparing the calculated frequencies of the ground state of C_2H_4 and C_2D_4 with the observed ones, we notice that the calculated values are overestimated by 8.6%–12.0%. The present result of the $^2B_{3u}$ state is in good agreement with the calculated value by Somasundran *et al.*[9] [see Tables V(a) and V(b)].

Tables VI(a) and VI(b) give the zero-point vibrational energies (ZPVEs), zero–zero ionization energies (0–0 IEs) and FCFs of the 0–0 transitions of the ionic states of C_2H_4 and C_2D_4, respectively. The calculated 0–0 IEs are com-

TABLE III. Vertical ionization energies (VIEs).

State	SCF Energy (a.u.)	SCF VIE (eV)	SDCI Energy (weight) (a.u.) (%)	SDCI VIE (eV)	QC[a] VIE (eV)
^1A_g	−78.061 176	0.0	−78.365 105(90)	0.0	
$^2B_{3u}$	−77.728 089	9.06	−77.987 974(92)	10.26	10.51
$^2B_{3g}$	−77.580 030	13.09	−77.882 921(89)	13.12	13.06
^2A_g	−77.526 581	14.55	−77.818 189(90)	14.88	14.87
$^2B_{2u}$	−77.444 461	16.78	−77.754 886(88)	16.60	16.41
$^2B_{1u}$	−77.296 319	20.81	−77.627 751(86)	20.06	19.64

[a] QC: Corrected energy of quadruple excitations by Lnaghoff and Davidson's (Ref. 18) method.

TABLE IV. Adiabatic ionization energies (AIEs).

State	SCF Energy (a.u.)	SCF AIE (eV)	SDCI Energy (weight) (a.u.) (%)	SDCI AIE (eV)	QC AIE (eV)
^1A_g	−78.061 176	0.0	−78.365 105(90)	0.0	0.0
$^2B_{3u}$	−77.736 221	8.84	−77.997 389(92)	10.01	10.23
$^2B_{3g}$	−77.602 881	12.47	−77.901 927(90)	12.60	12.57
^2A_g	−77.563 549	13.54	−77.853 924(89)	13.91	13.88
$^2B_{2u}$	−77.470 002	16.09	−77.780 077(88)	15.92	15.70
$^2B_{1u}$	−77.320 745	20.15	−77.647 431(87)	19.53	19.15

TABLE V. Vibrational energies (cm^{-1}) of (a) $C_2H_4^+$ and (b) $C_2D_4^+$.

(a) Mode	State ^1A_g Calc.	^1A_g Expt.[a]	$^2B_{3u}$	$^2B_{3g}$	^2B_g	$^2B_{2u}$	$^2B_{1u}$
ν_1	3292	3026	3292	3039	3174	2944	2755
ν_2	1818	1623	1694(1694)[b]	1922	1579	1706	1967
ν_3	1478	1342	1358(1362)	1222	1199	1404	1367

(b) Mode	State ^1A_g Calc.	^1A_g Expt.[a]	$^2B_{3u}$	$^2B_{3g}$	^2A_g	$^2B_{2u}$	$^2B_{1u}$
υ_1	2443	2251	2418	2456	2267	2275	2154
υ_2	1679	1515	1484(1487)[b]	1680	1326	1538	1764
υ_3	1079	981	1056(1057)	866	1000	1008	976

[a] Herzberg (Ref. 23).
[b] Calculated value by Somasundran *et al.* (Ref. 9).

TABLE VI. 0–0 ionization levels of (a) C_2H_4 and (b) C_2D_4.

(a) State	ZPVE[a] (eV)	0–0 IE[b] (eV) SDCI	QC	obs.[d]	FCF[c]
^1A_g	0.41	...	...	...	
$^2B_{3u}$	0.39	10.00	10.22	10.51	0.322
$^2B_{3g}$	0.38	12.58	12.55	12.46	0.079
^2A_g	0.37	13.87	13.84	14.46	0.006
$^2B_{2u}$	0.38	15.89	15.67	15.78	0.043
$^2B_{1u}$	0.38	19.50	19.12	18.87	0.092

(b) State	ZPVE[a] (eV)	0–0 IE[b] (eV) SDCI	QC	obs.[d]	FCF[c]
^1A_g	0.32	...	...	...	
$^2B_{3u}$	0.31	10.00	10.22	10.52	0.313
$^2B_{3g}$	0.31	12.59	12.56	12.48	0.041
^2A_g	0.29	13.87	13.84	14.45	0.002
$^2B_{2u}$	0.30	15.90	15.68	15.83	0.012
$^2B_{1u}$	0.30	19.51	19.13	18.90	0.038

[a] ZPVE: Zero-point vibrational energy.
[b] 0–0 IE: 0–0 ionization energy.
[c] FCF: Franck–Condon factor.
[d] Reference 2.

pared with the observed values. The calculated 0–0 IEs of the $^2B_{3u}$, $^2B_{3g}$, and $^2B_{1u}$ states obtained by the QC method give better agreement with the observed values than those by the SDCI method.

Using the 0–0 IEs from the QC energies and vibrational frequencies and FCFs, we obtained the theoretical intensity curves of ionization by assuming a halfwidth of 0.08 eV for each transition band. The results of C_2H_4 and C_2D_4 are illustrated in Fig. 2 and Fig. 3, respectively. They are compared with the observed PE spectrum by Branton *et al.*[2] in Fig. 2 and Fig. 3. The theoretical intensity curves of the first and fourth ionic states of C_2H_4 are in good agreement with the observed PE spectrum. The theoretical intensity curve of the second and third band shows well resolved vibrational structure, whereas the observed band is not as completely resolved as the calculated ones. The present approach to the second and third band fails to reproduce the observed band shape. In order to see more detailed vibrational structure, we illustrate the theoretical intensity curve with a halfwidth of 0.02 eV for each state. The theoretical intensity curves for the $^2B_{3u}$ state of C_2H_4 and C_2D_4 are illustrated in Fig. 4 and Fig. 5, respectively. Those for the $^2B_{3g}$, ^2A_g, $^2B_{2u}$, and $^2B_{1u}$ states are illustrated in Fig. 6, Fig. 7, Fig. 8, and Fig. 9, respectively.

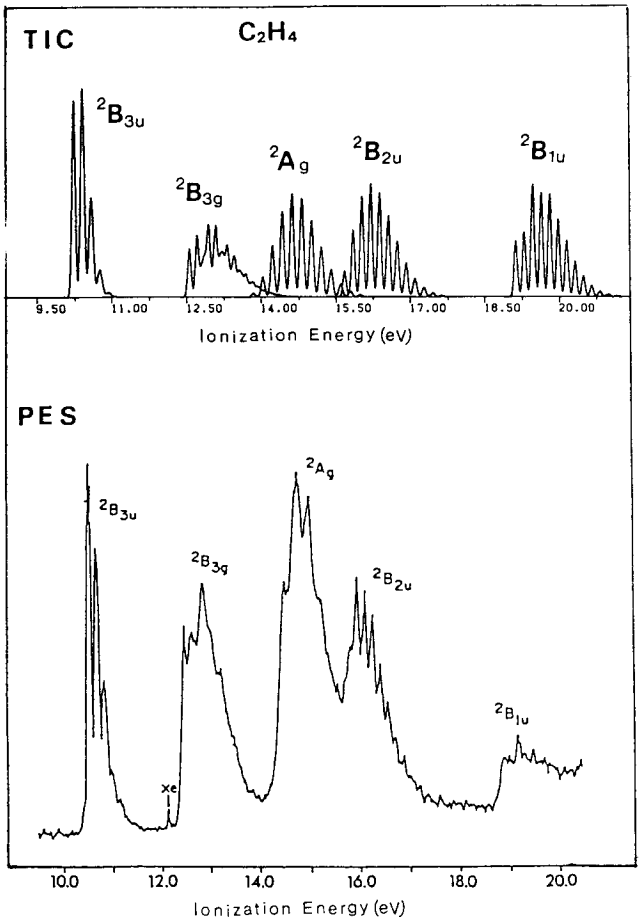

FIG. 2. The theoretical intensity curves of ionization of C_2H_4 assuming a halfwidth of 0.08 eV, which is compared with the observed PE spectrum by Branton *et al.* (Ref. 2). TIC: Theoretical intensity curve; PES: PE spectrum.

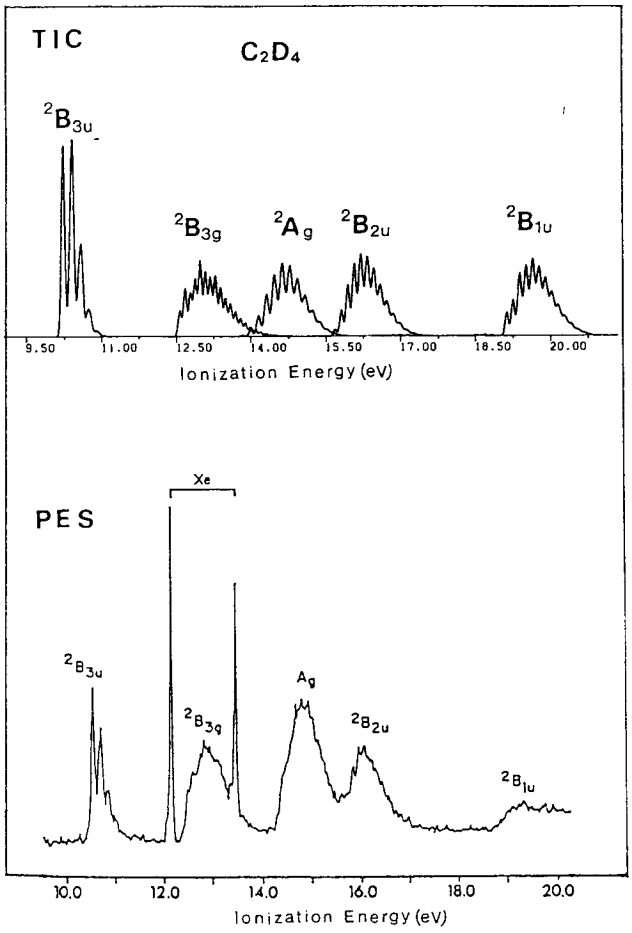

FIG. 3. The theoretical intensity curves of ionization of C_2D_4 assuming a halfwidth of 0.08 eV, which is compared with the observed PE spectrum by Branton *et al.* (Ref. 2) TIC: Theoretical intensity curve; PES: PE spectrum.

A. First ionic state ($^2B_{3u}$)

Figure 4 shows the theoretical intensity curve of ionization of C_2H_4 to $^2B_{3u}$, which is compared with the observed PE spectrum by Pollard *et al.*[5] The observed PE spectrum shows the doubling of each peak by the torsional mode (ν_4 mode). However, the present theoretical intensity curve does not include the contribution of the torsional vibrational mode. Because the torsional potential function has double minima, it is impossible to estimate the contribution of the torsional vibrational mode within the framework of the harmonic oscillator approximation. Therefore, we disregared the contribution of the torsional vibrational mode. Köppel *et al.*[13] have reported the vibronic coupling effects of the first ionic state and concluded that nonadiabatic effects were small. The present results also show that the adiabatic approximation appropriately describes the vibrational energy levels of the first ionic state. Three vibrational progressions (A, B, and C) are found in the theoretical intensity curve and the vibrational levels are assigned in parentheses where the vibrational quantum numbers of the ν_1, ν_2, and ν_3 modes are

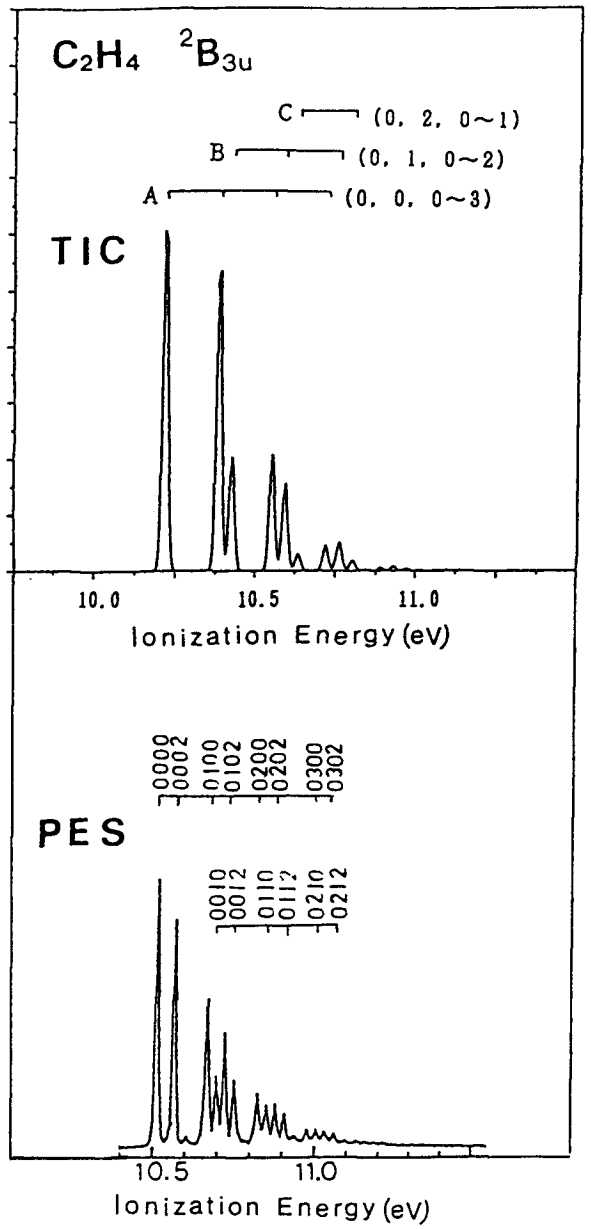

FIG. 4. The theoretical intensity curve of ionization of $^2B_{3u}$ of C_2H_4 with a halfwidth of 0.02 eV (not including the torsional ν_4 mode), which is compared with the observed PE spectrum by Pollard *et al.* (Ref. 5). The observed PE spectrum appears the doubling of each peak by the ν_4 mode.

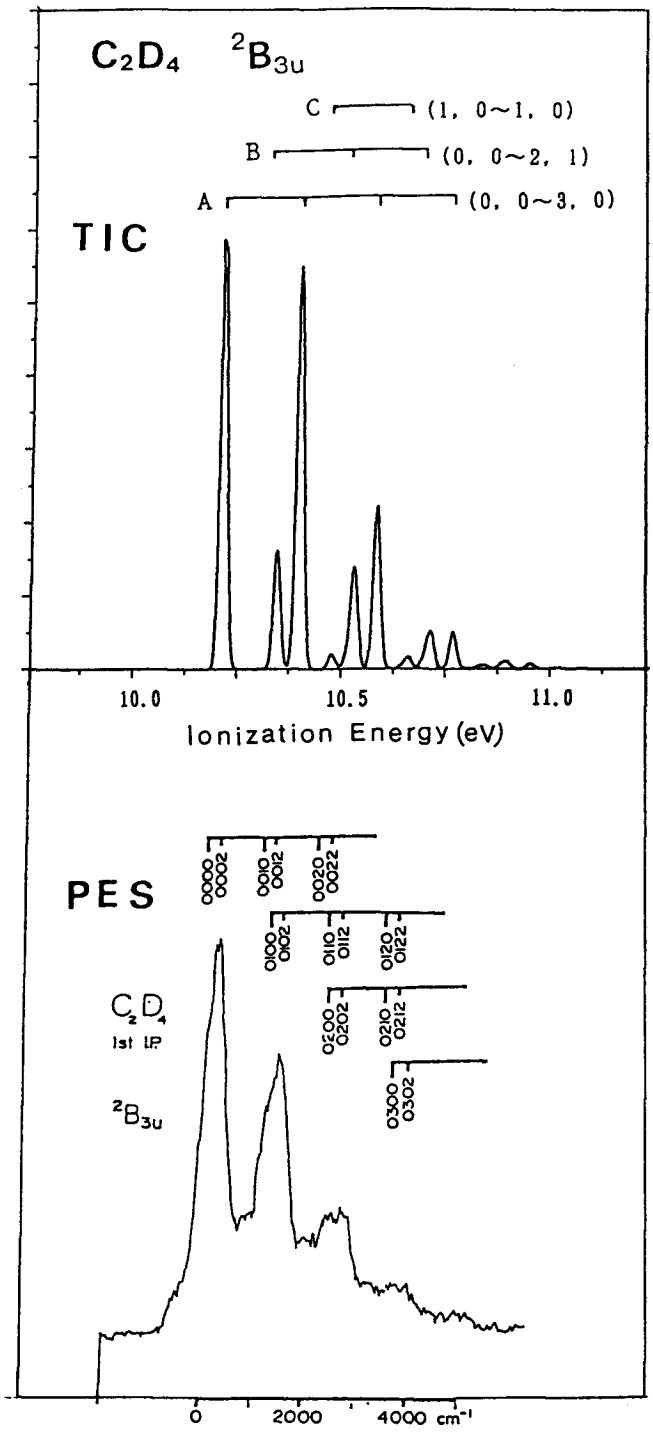

FIG. 5. The theoretical intensity curve of ionization of $^2B_{3u}$ of C_2D_4 with a halfwidth of 0.02 eV, which is compared with the observed PE spectrum by Branton *et al.* (Ref. 1).

listed. The progressions *A*, *B*, and *C* have strong, middle, and weak intensity, respectively. The progression *A* consists of the vibrational excitations of the ν_3 ($v_3 = 0$–3) mode and the progression *B* consists those of the ν_2 ($v_2 = 1$) and ν_3 ($v_3 = 0$–2) modes. In order to characterize each normal mode, a classical half-amplitude of the zero-point vibration of the $^2B_{3u}$ state was calculated. The result is shown in Table VII. This table reveals that the C–C stretching is strongly coupled with the H–C–H bending motion in the ν_2 and ν_3 modes. The phase of the linear combination of the C–C stretching and H–C–H bending is in phase for the ν_2 mode and out of phase for the ν_3 mode. Although a strong coupling of the C–C stretching and H–C–H bending is found in the ν_2 and ν_3 modes, we notice that the C–C stretching motion is dominant in the ν_3 mode. Thus we may assign the ν_3 mode to the C–C stretching mode and the ν_2 mode to the H–C–H bending mode. Pollard *et al.* assigned the major vibrational progression, which corresponds to our progression *A*, to the excitations of the C–C stretching mode (ν_2 mode by their notation). This is consistent with our result. The observed vibrational frequencies of the C–C stretching and the H–C–H bending modes by Pollard *et al.*[5] are 1260 and 1494

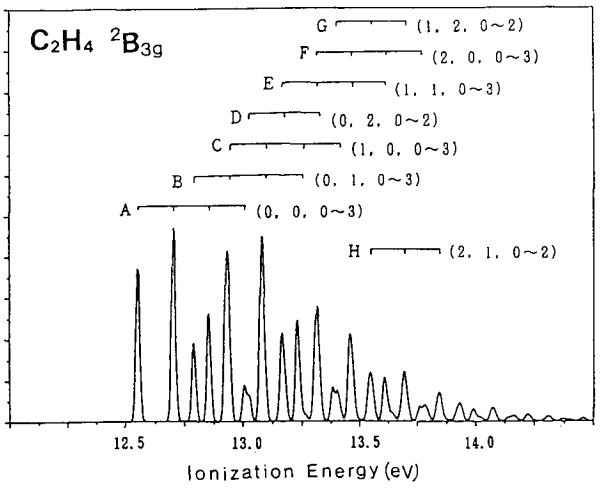

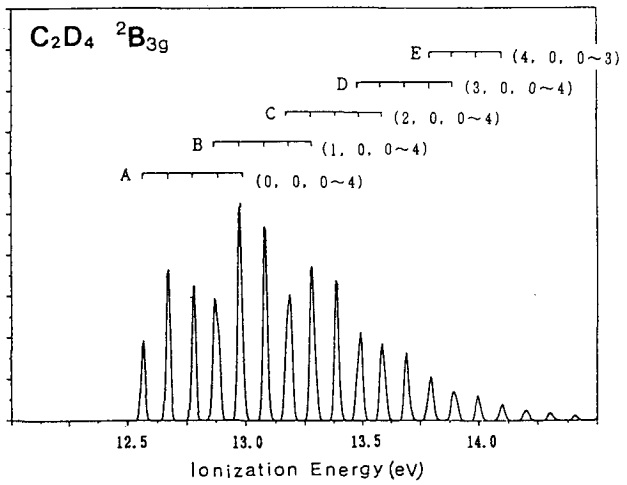

FIG. 6. The theoretical intensity curve of ionization of $^2B_{3g}$ C_2H_4 and C_2D_4 with a halfwidth of 0.02 eV.

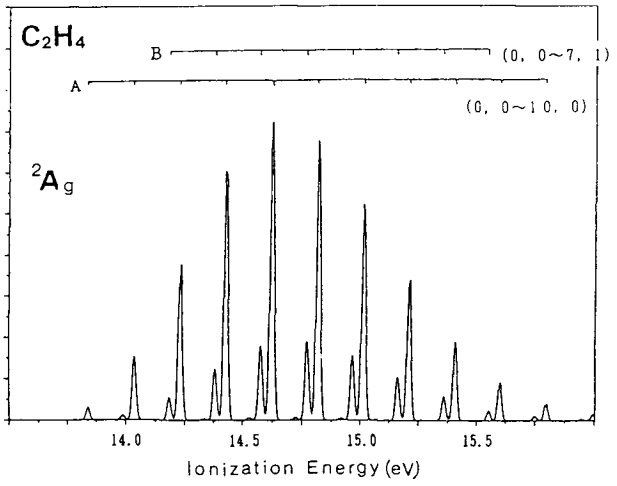

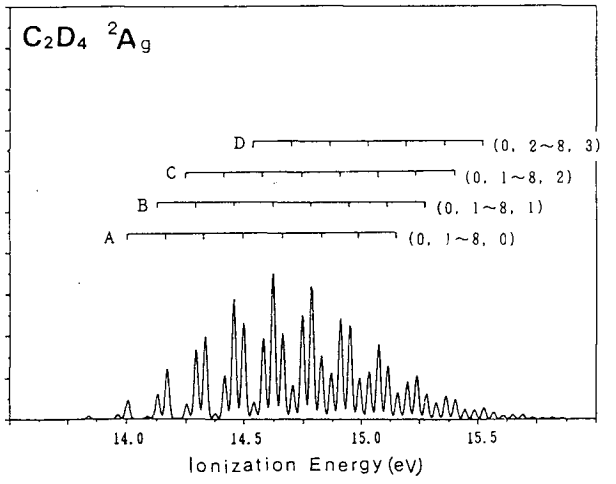

FIG. 7. The theoretical intensity curve of ionization of ^2A_g C_2H_4 and C_2D_4 with a halfwidth of 0.02 eV.

cm^{-1}, respectively. The calculated values of the C–C stretching and the H–C–H bending overestimate by 7.8% and 13.4%, respectively. The accuracy of the present calculation is the same order as that of the ground state.

Figure 5 shows the theoretical intensity curve of ionization of C_2D_4 to $^2B_{3u}$, which is compared with the observed PE spectrum by Branton *et al.*[1] The vibrational structure of the theoretical curve is in good agreement with the observed PE spectrum. Three vibrational progressions are included in the theoretical intensity curve: progression *A* of strong intensity; progression *B* of intermediate intensity; and progression *C* of weak intensity. Progression *A* consists of vibrational excitations of the ν_2 ($v_2 = 0$–3) mode and progression *B* consists those of the ν_2 ($v_2 = 0$–2) and ν_3 ($v_3 = 1$) modes. Table VII gives also the classical half-amplitude of the zero-point vibration of the $^2B_{3u}$ state of C_2D_4. This table reveals that the C–C stretching is mixed with the H–C–H bending motion in the ν_2 and ν_3 modes. The phase of the linear combination of the C–C stretching and H–C–H bending is in phase for the ν_2 mode and out of phase for the ν_3 mode. Using the same procedure as in C_2H_4, we may assign the ν_2 mode to the C–C stretching mode and the ν_3 mode to the H–C–H bending mode. Thus we should assign progression *A* to excitation of the C–C stretching mode. Branton *et al.*[1] have assigned the major vibrational progression, which corresponds to progression *A*, to excitation of the H–C–H bending mode. This does not agree with our result. They proposed that the observed vibrational frequencies of the C–C stretching and the H–C–H bending modes are 1200 ± 30 and $1100 \pm 100\ cm^{-1}$, respectively. The calculated values of the ν_2 and ν_3 modes are 1484 and 1056 cm^{-1}, respectively. The calculated values of the C–C stretching overestimate by $23.7 \pm 3\%$ and that of the H–C–H bending underestimate by $4.0 \pm 8\%$. These errors are beyond the accuracy of the present calculation. Therefore, Branton *et al.* may be missing the assignment of the vibrational progression.

B. Second ionic state ($^2B_{3g}$)

The theoretical intensity curve of ionization of C_2H_4 to $^2B_{3g}$ is illustrated in Fig. 6. It shows well resolved vibrational structure, whereas the observed band by Turner *et al.*[3] shows

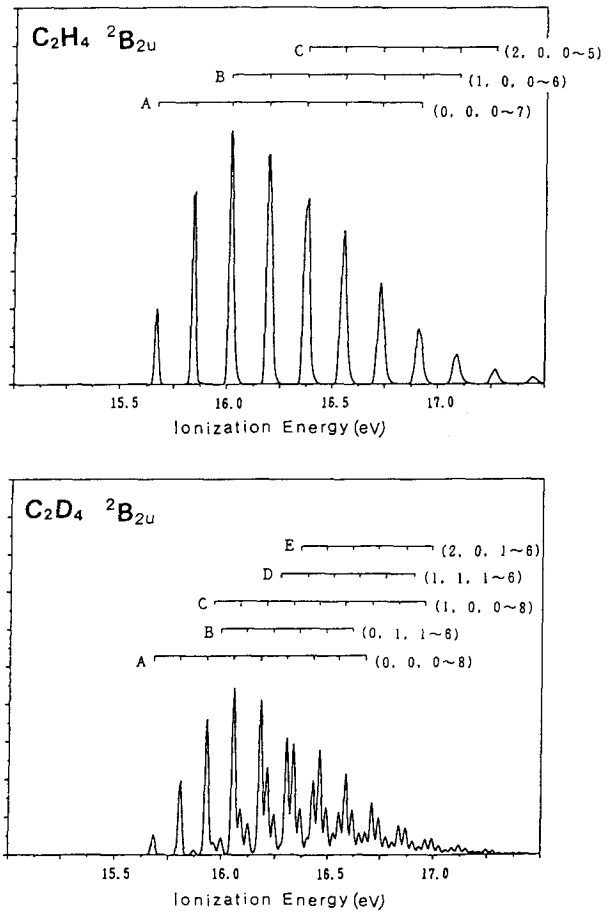

FIG. 8. The theoretical intensity curve of ionization of $^2B_{2u}$ C_2H_4 and C_2D_4 with a halfwidth of 0.02 eV.

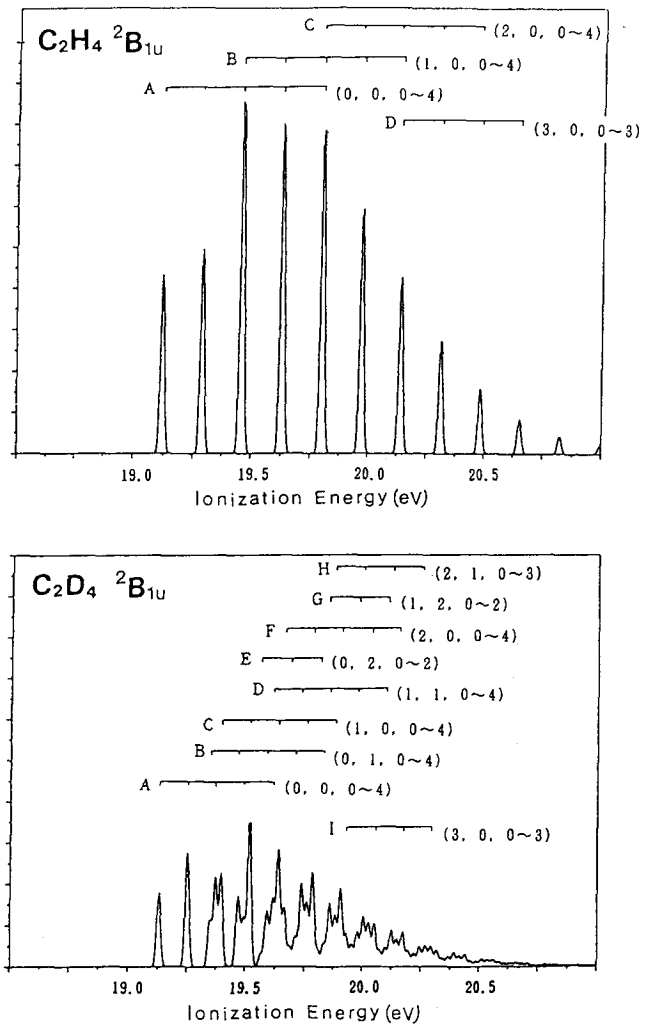

FIG. 9. The theoretical intensity curve of ionization of $^2B_{1u}$ C_2H_4 and C_2D_4 with a halfwidth of 0.02 eV.

broad character. Köppel *et al.*[14] have studied the nonadiabatic effects in this state that result in strong vibronic coupling with the first state. They succeeded in explaining the broad character of the band. They concluded that the broad bumps observed in the spectrum are accumulations of many vibronic lines (more than 1000 calculated lines) and assignment in terms of vibrational quantum numbers is impossible in principle. Because the adiabatic approximation is inadequate for this state, we should abandon further discussion based on the adiabatic approximation.

C. Third ionic state (^2A_g)

Figure 7 shows the theoretical intensity curve of ionization of C_2H_4 to ^2A_g. The figure shows only two vibrational progressions: progression A of strong intensity due to the excitation of the ν_2 ($v_2 = 0$–10) mode and progression B due to the excitation of the ν_2 ($v_2 = 0$–7) and ν_3 ($v_3 = 1$) modes. The classical half-amplitude of the zero-point vibrations (see Table VIII) indicates that the ν_2 mode is assigned to the H–C–H bending mode and the ν_3 mode to the C–C stretching. Excitations of the ν_2 and ν_3 modes are connected with the large change of geometry in the H–C–H angle (+ 24.0°) and in the C–C bond length (+ 0.115 Å), respectively.

The theoretical intensity curve of ionization of C_2D_4 to ^2A_g is shown in Fig. 7, where five vibrational progressions are presented. Progression B ($v_2 = 1$–8, $v_3 = 1$) has strong intensity and the progressions A ($v_2 = 1$–8, $v_3 = 0$) and C ($V_2 = 1$–8, $v_3 = 2$) have medium intensity. All progressions are due to the excitation of the ν_2 and ν_3 modes. The classical half-amplitude of the zero-point vibration given in Table VIII shows that the H–C–H bending motion is mixed with the C–C stretching motion in the ν_2 and ν_3 modes. The phase of the linear combination of the H–C–H bending and C–C

TABLE VII. Classical half-amplitude of the $^2B_{3u}$ state.[a]

	Vibrational mode		
	ν_1	ν_2	ν_3
C–C	− 0.010	− 0.035	0.049
C–H	0.051	− 0.002	0.003
H–C–H	− 0.4	− 7.5	− 3.0
C–C	− 0.021	− 0.053	0.022
C–D	0.043	− 0.008	0.002
D–C–D	− 1.0	− 4.3	− 5.3

[a] Bond lengths are in angstroms, angles in degrees.

TABLE VIII. Classical half-amplitude of the ^2A_g state.[a]

	Vibrational mode		
	ν_1	ν_2	ν_3
C–C	− 0.005	− 0.027	0.061
C–H	0.052	0.004	0.001
H–C–H	0.0	− 8.3	− 0.9
C–C	− 0.011	− 0.057	0.032
C–D	0.044	− 0.000	0.003
D–C–D	− 0.4	− 5.5	− 4.6

[a] Bond lengths are in angstroms, angles in degrees.

stretching is in phase for the ν_2 mode, which is consistent with the change in equilibrium geometry by ionization. Thus the ν_2 mode should contribute mainly to the intensity.

The theoretical intensity curves both C_2H_4 and C_2D_4 fail to reproduce the observed spectra which are more broadband. As was pointed by Pollard *et al.*,[5] the nonadiabatic effects should be important.

D. Fourth ionic state ($^2B_{2u}$)

In Fig. 8, we show the theoretical intensity curve of ionization of C_2H_4 to $^2B_{2u}$ which appears 11 well-resolved peaks with a spacing of about 1400 cm^{-1}. The figure mimics well the observed PE spectrum by Pollard *et al.*[5] who found at least 11 resolved peaks and that the average of the first six peaks splitting is 1245 ± 20 cm^{-1}. The calculated spacing overestimates the observed one by 12.2%. Branton *et al.*[1,2] have assigned this progression due to the excitation of the ν_2 (C–C stretching) and ν_3 (H–C–H bending) modes. Pollard *et al.* assigned it to the excitation of the ν_2 mode. They also interpreted this state as a clear example of vibrational structure at a saddle point in the potential surface based on the result of the calculation by Sannen *et al.*[11] However, the present calculation of the potential surface vs torsional angle shows that the planar molecular structure is stable and the theoretical intensity curve is very similar to the observed PE spectrum. Therefore, we do not need an idea of the vibrational structure at a saddle point. The vibrational levels are illustrated in Fig. 8 where three progressions are found: progressions A ($v_1 = 0$, $v_3 = 0$–7), B ($v_1 = 1$, $v_3 = 0$–6), and C ($v_1 = 2$, $v_3 = 0$–5). These progressions are due to the excitation of the ν_1 and ν_3 modes and not the ν_2 mode. The classical half-amplitude of the zero-point vibration is given in Table IX. The results show that the ν_1, ν_2, and ν_3 modes are assigned to the C–H stretching, C–C stretching, and H–C–H bending modes, respectively. Vibrational excitations of the C–H stretching and H–C–H bending modes are connected with the large change in the geometry of the C–H bond distance (+ 0.060 Å) and the H–C–H angle (− 16.7°). Although two modes of different vibrational frequencies (2944 cm^{-1} of ν_1 and 1404 cm^{-1} of ν_3) contribute to the progressions, the theoretical intensity curve has well-resolved vibrational structure. This feature can be explained by observing that the vibrational frequency of the ν_1 mode is almost twice that of the ν_3 mode.

The theoretical intensity curve of ionization of C_2D_4 to $^2B_{2u}$ is illustrated in Fig. 8. Five progressions are found in the theoretical intensity curve and the vibrational levels are shown in parentheses. Progressions A ($v_3 = 0$–8) has strong intensity at the lower energy side. Progression C ($v_1 = 1$, $v_3 = 0$–8) has strong intensity at the higher energy side. The classical half-amplitude of the zero-point vibration is given in Table IX. The results show that the ν_1, ν_2, and ν_3 modes are the C–D stretching, C–C stretching, and D–C–D bending modes, respectively. The calculated vibrational frequencies of the ν_1 and ν_3 modes are 2275 and 1008 cm^{-1}, respectively. The vibrational structure of the theoretical intensity curve and the observed PE spectrum does not resolve as well as that of C_2H_4. The reason is that the relation $\nu_1 \simeq 2\nu_3$ does not hold for C_2D_4.

E. The fifth ionic state ($^2B_{1u}$)

Figure 9 shows the theoretical intensity curve of ionization of C_2H_4 to $^2B_{1u}$. The figure reveals five vibrational progressions. Progressions A ($v_3 = 0$–4) and B ($v_1 = 1$, $v_3 = 0$–4) have strong intensity and progression C ($v_1 = 2$, $v_3 = 0$–4) has intermediate intensity. The excitations of the ν_1 and ν_3 modes contribute to all progressions. Well-resolved vibrational structure of the theoretical intensity curve is ascribed to the relation between vibrational frequencies of the ν_1 (2755 cm^{-1}) and ν_3 (1367 cm^{-1}) modes ($\nu_1 \simeq 2\nu_3$). The classical half-amplitude of the zero-point vibration is given in Table X. This table indicates that the ν_1 and ν_3 modes are assigned to the C–H stretching and H–C–H bending modes,

TABLE IX. Classical half-amplitude of the $^2B_{2u}$ state.[a]

	Vibrational mode		
	ν_1	ν_2	ν_3
C–C	− 0.016	− 0.050	0.021
C–H	0.055	− 0.008	0.002
H–C–H	− 0.7	− 4.4	− 6.5
C–C	− 0.033	0.045	0.009
C–D	0.043	0.020	0.001
D–C–D	− 1.5	2.4	− 6.1

[a] Bond lengths are in angstroms, angles in degrees.

TABLE X. Classical half-amplitude of the $^2B_{1u}$ state.[a]

	Vibrational mode		
	ν_1	ν_2	ν_3
C–C	− 0.013	− 0.050	0.014
C–H	0.056	− 0.006	0.005
H–C–H	− 0.4	− 3.8	− 6.9
C–C	− 0.041	0.033	0.008
C–D	0.035	0.032	0.004
D–C–D	− 2.0	2.1	− 6.1

[a] Bond lengths are in angstroms, angles in degrees.

respectively. Excitations of the ν_1 and ν_3 modes are connected with the large change of geometry in the C–H bond length (+ 0.078 Å) and the H–C–H angle (+ 10.06°).

The theoretical intensity curve of ionization of C_2D_4 to $^2B_{1u}$ is shown in Fig. 9, where nine vibrational progressions are found. The excitation of the ν_1, ν_2, and ν_3 modes contribute to intensity. The classical half-amplitude of the zero-point vibration given in Table X. It shows that the C–D stretching is mixed with the C–C stretching motion in the ν_1 and ν_2 modes. The phase of the linear combination of the C–D stretching and the C–C stretching is out of phase for the ν_1 mode and in phase for the ν_2 mode. The ν_3 mode is assigned to the D–C–D bending mode.

IV. CONCLUSION

The molecular equilibrium structure and vibrational frequencies are calculated for the ground and lower five ionic states. By the use of the FCFs, we obtain the transition intensity curve. The summary of results are as follows.

A twisted equilibrium structure of the lowest ionic state ($^2B_{3u}$) is obtained only by including a quadruple correction. The equilibrium structures of the $^2B_{3g}$, ^2A_g, $^2B_{2u}$, and $^2B_{1u}$ states are planar.

Within the framework of the adiabatic approximation and the harmonic oscillator approximation, the theoretical intensity curve is calculated. For the first ionic state ($^2B_{3u}$), the theoretically calculated excitation of the totally symmetric modes is in good agreement with the observed PE spectrum. The vibrational structure of the theoretical intensity curve of the fourth ionic state ($^2B_{2u}$) is in agreement with the observed PE spectrum. However, the second and third band (^2A_g) fail to reproduce the observed band shape. Non-adiabatic effects should be important in both states.

For the fourth ionic state ($^2B_{2u}$), the planar molecular structure is stable. The well-resolved vibrational structure of the theoretical intensity curve of $C_2H_4^+$ mimics well the PE spectrum. The vibrational excitation of the ν_3 mode (H–C–H bending motion) contributes mainly intensity.

For the fifth ionic state ($^2B_{1u}$), the excitation of the ν_1 and ν_3 modes contribute to the intensity. The ν_1 mode is assigned to the C–H stretching and the ν_3 mode is the H–C–H bending mode.

ACKNOWLEDGMENTS

The author wishes to thank Dr. K. Tanaka for reading the manuscript and helpful discussions. He would like to thank Professor F. Sasaki for useful suggestions. Computations were was carried out on HITAC M-680H systems at the Center for Information Processing Education of Hokkaido University.

[1] G. R. Branton, D. C. Frost, T. Makita, C. A. McDowell, and I. A. Stenhouse, J. Chem. Phys. **52**, 802 (1970).
[2] G. R. Branton, D. C. Frost, T. Makita, C. A. McDowell, and I. A. Stenhouse, Phil. Trans. R. Soc. London Ser. A **268**, 77 (1970).
[3] D. W. Turner, A. D. Baker, C. Baker, and C. R. Brundel, *Molecular Photoelectron Spectroscopy* (Wiley-Interscience, London, 1970).
[4] K. Kimuara, S. Katsumata, Y. Achiba, T. Yamazaki, and S. Iwata, *Handbook of HeI Photoelectron Spectra of Fundamental Organic Molecules* (Halsted, New York, 1981).
[5] J. E. Pollard, D. J. Trevor, J. E. Reutt, Y. T. Lee, and D. A. Shirley, J. Chem. Phys. **81**, 5302 (1984).
[6] P. M. Dehmer and J. L. Dehmer, J. Chem. Phys. **70**, 4575 (1979).
[7] W. A. Lathan, W. J. Hehre, and J. A. Pople, J. Am. Chem. Soc. **93**, 808 (1975).
[8] W. R. Rodwell, M. F. Guest, D. T. Clark, and D. Shuttleworth, Chem. Phys. Lett. **45**, 50 (1977).
[9] K. Somasundram and N. C. Handy, J. Chem. Phys. **84**, 2899 (1985).
[10] S. Merry and C. Thomson, Chem. Phys. Lett. **82**, 373 (1981).
[11] C. Sannen, G. Raseev, C. Gallory, G. Fauville, and J. C. Lorquet, J. Chem. Phys. **74**, 2402 (1981).
[12] N. C. Handy, R. H. Nobes, and H. J. Werner, **110**, 459 (1984).
[13] H. Köppel, W. Domcke, L. S. Cederbaum, and W. von Niessen, J. Chem. Phys. **69**, 4252 (1978).
[14] H. Köppel, L. S. Cederbaum, and W. Domcke, J. Chem. Phys. **77**, 2014 (1982).
[15] F. B. van Duijneveldt, IBM Research Report RJ 945 (1971).
[16] T. Shoda, D. Sc. thesis, Hokkaido University, 1989.
[17] A. D. Mclean and B. Liu., J. Chem. Phys. **58**, 1066 (1973).
[18] S. R. Langhoff and E. R. Davidson, Int. J. Quantum Chem. **8**, 61 (1974).
[19] T. Shoda, T. Noro, T. Nomura, and K. Ohno, Intern. J. Quantum Chem. **30**, 289 (1986).
[20] K. Takeshita, J. Chem. Phys. **86**, 329 (1987).
[21] K. Takeshita and F. Sasaki, 1981 Library program at the Hokkaido University Computing Center (in Japanese). GRAMOL included the program JAMOL3 of the RHF calculation written by H. Kashiwagi, T. Takada, E. Miyoshi, and S. Obara for the Library program at the Hokkaido University Computing Center 1977 (in Japanese).
[22] A. Murakami, H. Iwaki, H. Terashima, T. Shoda, T. Kawaguchi, and T. Noro 1986 Library program at the Hokkaido University Computing Center (in Japanese).
[23] G. Herzberg, Electronic Spectra of Polyatomic Molecules, D. Van Nostrand Company.